PRELIMINARY DESIGN OF MORPHING FLAPERON USING OPTIMIZATION BY GENETIC ALGORITHM

Lukáš Dubnický[1], Jaroslav Juračka[1], Jan Šplíchal[1], František Löffelmann[1] & Jaroslav Bartoněk[1]

[1]Institute of Aerospace Engineering, Faculty of Mechanical Engineering, Brno University of Technology, Technická 2896/2, 616 69 Brno

Abstract

This article presents an approach to morphing flaperon design. The presented design workflow attempts a simple structural arrangement of trailing edge morphing for applicability in short-term. The concept of the integrated hinge with load-bearing upper skin was adapted in combination with the laminar airfoil. This substitutes the traditional hinged flaperon, bringing the performance benefits of continuous upper skin surface. The preliminary design focuses on the built-in of the morphing mechanism into the airfoil. The goal is to obtain the geometrical parameters that describe the arrangement features for the built-in. To meet the contrary requirements on stiffness and compliancy of the morphing structure, the design is performed as a multidisciplinary optimization problem which is solved using genetic algorithm. Parameters of the geometry that define the built-in features form the optimization input parameters. The objective function for optimization incorporates the reserve factor, target deflection and actuation force for both upper and lower deflection. To produce the single objective value a weighting accompanied with constraints is used. The described problem was solved using Matlab scripting, combined with structural Nastran finite element method solver to determine individual's properties for evaluation and selection. The problem formulation and design workflow fulfil the goal. The obtained set of parameters defines the morphing flaperon geometry, that allows achieving the described deflections with the required reserve factors, therefore verifying the morphing mechanism. The design workflow proved feasible and will be further developed.

Keywords: morphing, flaperon, optimization, genetic algorithm

1. Introduction

Airfoil morphing is the ability to change the cross-sectional profile of an aerodynamic surface, which may substitute traditional control surfaces and high-lift devices that use rotational, translational or combined movement. Many concepts emerged throughout the decades. Barbarino et al. [1] offered the complex review of the technology and Thill et al. focused on the morphing skins. [2] Some concepts change the shape of an airfoil along its full chord length like the concept of Peel et al. [3], while others only morph a part of an airfoil. The morphing of the smaller part of an airfoil is generally a substitution of the leading or the trailing edge devices on a regular wing structure. The advantage of this approach can be seen in simpler design and keeping of the standard wing structure which may help short-term applicability. Frequently revisited concept of this type is the substitution of the trailing edge control surface hinge with a continuous load bearing upper skin. The skin bends for the control surface deflection. This concept can be seen in the work of many authors throughout the years [4], [5], [6] and is still developed nowadays [7], [8]. However, the combination of such a concept with the modern laminar airfoil was not given much attention. In the morphing of the laminar airfoils and the sailplane design, the leading-edge morphing by Achleitner et al. [9], [10] is very recognizable.

Morphing concepts, that involve the elastic deformation of the structural parts, present a contrary structural requirement. Stiffness is required to maintain a specified shape, whereas compliance is necessary to reduce the actuation force of the morphing elements. Therefore, such a structural design is always a multidisciplinary problem and leads to a complex optimization problem.

2. Design

The proposed morphing flaperon uses the elastic load bearing upper skin which connects a rigid wing structure with a rigid flaperon as shown in Figure 1. The skin bends for flaperon deflection. The lower surface skin is split. The split is covered using a tape, which is a regular solution on control surfaces. Future design might involve elongating skin. At the lower surface, an actuation push/pull rod connects to the flaperon. The connection pin is guided in the straight slot/rail which is a part of the wing body. The slot/rail supports the vertical translational forces of the flaperon and distributes them to the main wing body.

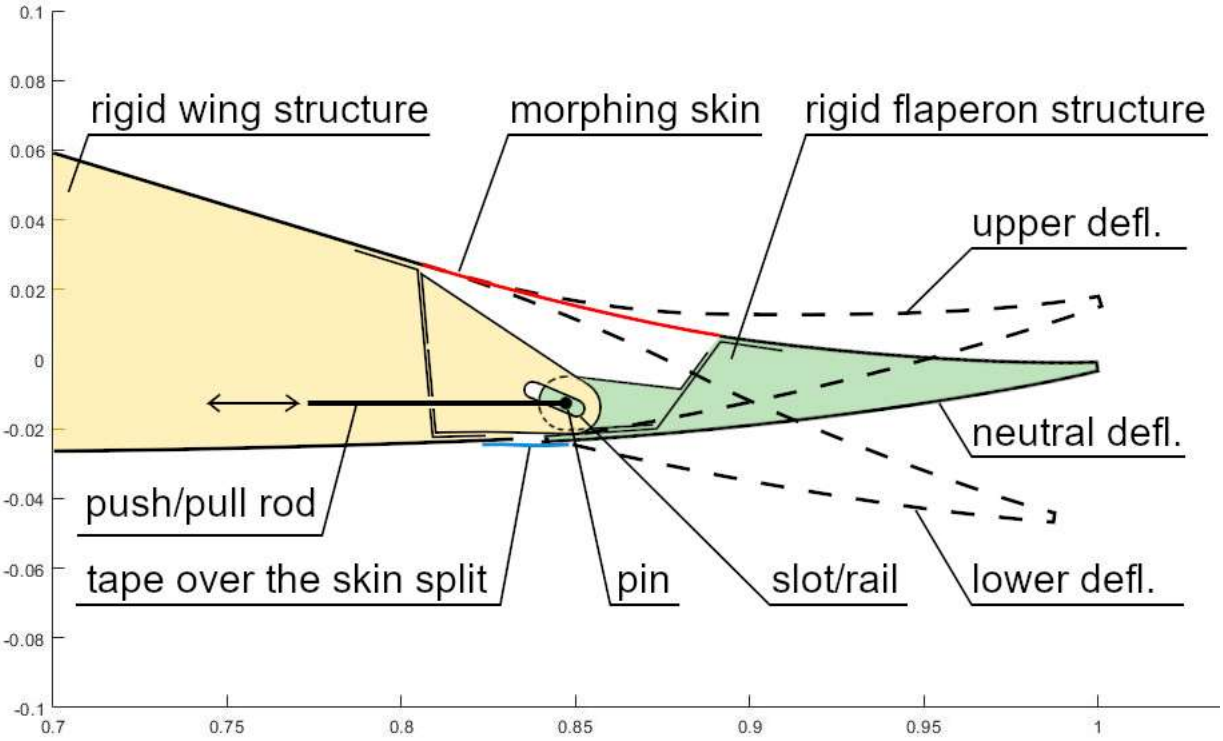

Figure 1 - Morphing flaperon structural arrangement on the airfoil trailing edge, unit lengths

The morphing upper skin is subjected to bending stress and strain during the deflections. Depending on the orientation of the deflection, it is also subjected to tensional load (for upper deflection) and compressive load (for lower deflection). These loads are formed as a reaction to the actuation force. This cannot be avoided as the force couple is necessary to create a flaperon deflection moment. In addition, the aerodynamic hinge moment adds to these forces and moments. It is assumed that dominant aerodynamic force acts against the flaperon deflection, therefore increasing the control force on the push/pull rod.

Considering the properties of the morphing skin, the control force required for flaperon deflection depends on the bending stiffness of the morphing skin. For the selected material with given elastic modulus, only the reduction of the morphing skin thickness can be used to reduce the control force. Lowering the skin thickness also lowers the bending stress at given deformation but it increases the axial stress, which is limited by required reserve factor. Therefore, an optimal skin thickness can be found.

Considering the geometry of the morphing flaperon, the morphing skin length and chordwise location is also subject to selection. The longer morphing skin allows higher flaperon deflections with lower strain as this can be distributed better. On the other hand, longer morphing skin carries higher aerodynamic loads and is susceptible to buckling issues. The slot incline (positive or negative) can be used to adjust the morphing skin loading in the motion and it can also influence the control force.

As can be seen, the selection of geometrical parameters is an optimization problem.

3. Method

As was described above, the shape definition of the airfoil offers several variables to geometrically optimize the flaperon built-in. The objective of the optimization is to receive the parameters for geometrical configuration that will enable reaching the selected flaperon deflection with suitable reserve factor with minimal control force for both upper and lower deflection.

For the preliminary design, the following simplification and assumptions are used. The only deforming part is the morphing skin, all other structural parts are considered to be rigid bodies. Aerodynamic verification of the final morphed shape is not present in this preliminary design to

reduce its complexity. Aerodynamic loads are simplified and estimated using the CS-23 acceptable means of compliance procedure.

The optimization workflow is tested on the modified Kubrynski kl-012-132f laminar airfoil. [11]

The sizing of the rigid parts and the elastic part of the airfoil is defined in a parametric way. It follows the design features for the morphing described above. The steps are illustrated in Figure 2.

- In the step 1, the 2 main geometrical parameters are set. Those are chord length ratios to split the rigid wing part from the morphing skin (e_x point) and to split the morphing skin from the rigid flaperon (f_x point). Where $f_x > e_x$. (Practical equivalent to length and chordwise location.)
- In the step 2, the morphing segment is geometrically bent down by selected deflection angle with assumed linear strain distribution. Linear strain distribution is assumed because such condition will be attempted by genetic algorithm in order to reduce skin stress and therefore maintain proper reserve factor. The rigid flaperon part is joined tangentially with morphing segment and follows it in the bending motion. In such motion the lower curve of the rigid flaperon intersects with the original lower curve of the airfoil. Above that intersection the hinge point is located, where the push/pull control rod connects to the rigid flaperon. The vertical distance is given by the minimum possible distance from the rigid flaperon lower skin based on the structure and need not to be optimized. For the preliminary design, this is assumed to be 0.5% of the chord length.
- In the step 3, the rail angle parameter (tan γ) is selected. The ability to set the rail angle allows to modify the morphing skin curve during the flaperon movement and redistributes the forces.

The corresponding structural geometry of the design is in the middle right position of Figure 2. The finite element method (FEM) model comprises of the isotropic morphing skin shell and the 3 rigid shells that substitute the rigid flaperon structure. The thickness of the morphing shell is the 4th optimization parameter. The fixed support is used where the morphing skin is connected to rigid wing structure. The sliding support models the rail connection of the flaperon and the wing. The control force is applied at this shell edge in the direction of the free movement. The orientation of the control force is selected in order to produce the upper or the lower deflection. In the bottom left-hand corner of Figure 2, the pushing control force is producing the upper deflection. In the bottom right-hand corner of Figure 2, the opposite orientation and deflection is shown. In both cases, the deflection of the flaperon is measured on the rigid part of the flaperon. The FEM model applies a control force, to reach the minimal deflection from the original airfoil contour.

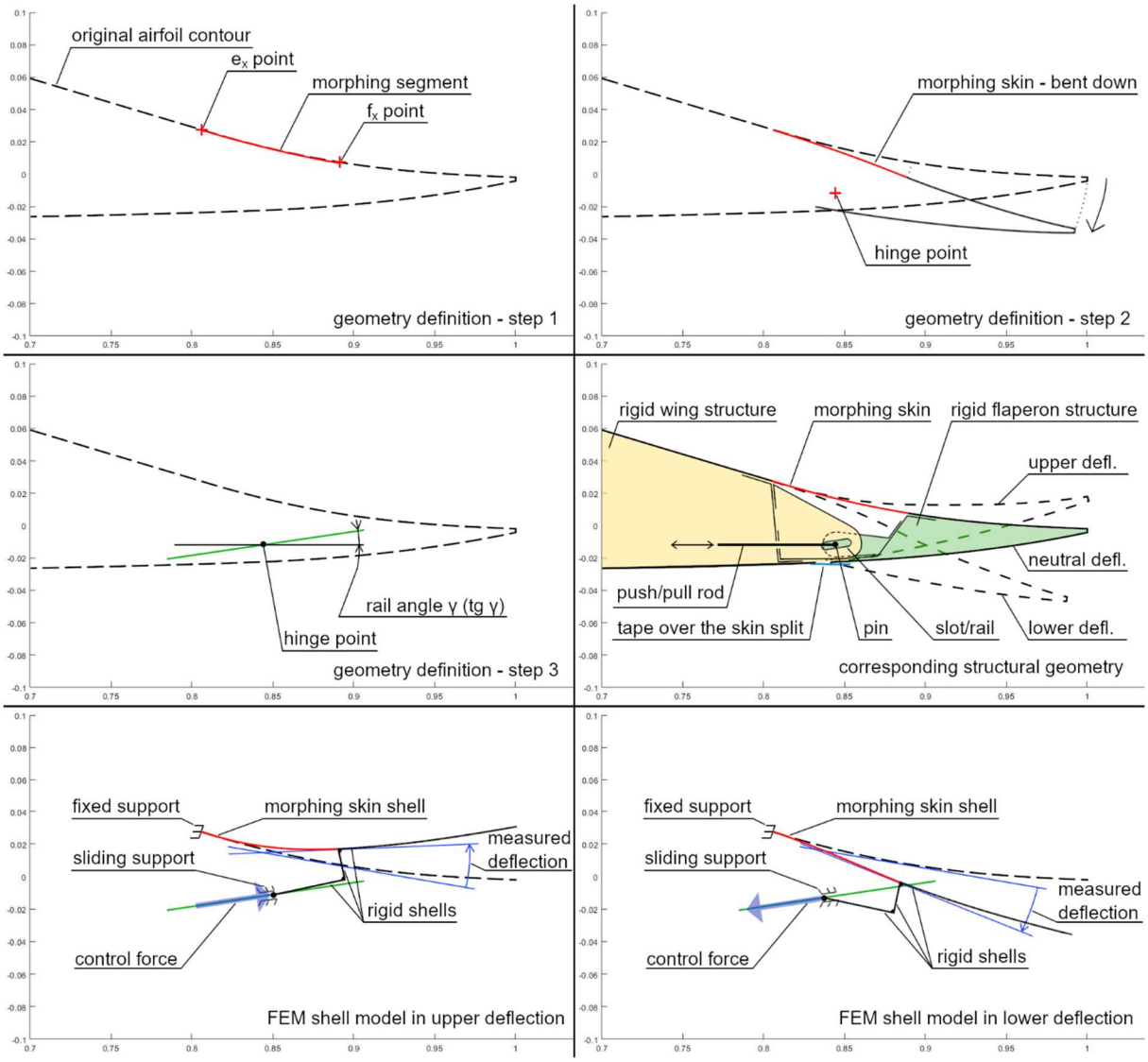

Figure 2 - Parametric geometry definition and FEM shell models in deflections

4. Optimization problem

Optimization objective is to achieve both the upper and lower deflection with appropriate reserve factor, with necessary deflection angles and with minimal control force. This presents a multicriteria optimization with 6 objective values, that is 3 for upper deflection, 3 for lower deflection. The objective values were combined using weighting. The weighting coefficients **{a}** have been chosen to give the final ratio approximately 1:1:1 between the 3 objective value groups. But the constraints for objective values have been added, which help to avoid impractical solutions with unnecessarily low RF. This was intended to reduce the impact of arbitrary weighting factors and created the sequence in satisfying the objectives as follows: 1. reserve factor - RF, 2. deflection angle - $\delta_{up,down}$ 3. control force – $q_{c\ up,\ down}$.

Objective function does not achieve a better result by further reduction of reserve factor values and deflection angles beyond the set threshold values. Therefore, it is possible to set the reserve factor value and deflection angle and any further reduction potential is then used to reduce the control force.

Therefore, the optimization problem can be written as:

$$\min_{\mathbf{x}\in\mathbf{P}}\left\{\mathrm{f} = \mathrm{a}_1\widehat{\mathrm{RF}}_{\mathrm{up}}(\mathbf{x}) + \mathrm{a}_1\widehat{\mathrm{RF}}_{\mathrm{down}}(\mathbf{x}) + \mathrm{a}_2\mathrm{q}_{\mathrm{c\,up}}(\mathbf{x}) + \mathrm{a}_2\mathrm{q}_{\mathrm{c\,down}}(\mathbf{x}) + \mathrm{a}_3\mathrm{k}_{\mathrm{up}}(\mathbf{x}) + \mathrm{a}_3\mathrm{k}_{\mathrm{down}}(\mathbf{x})\right\} \quad (1)$$

where objective function f is not reduced by reducing $RF_{up,down}$ under the threshold of 0.5 therefore:

$$\widehat{\mathrm{RF}}_{\mathrm{up,down}} = \begin{cases} 0.5 \;\; if \; RF_{up,down} \leq 0.5 \\ RF_{up,down} \;\; otherwise \end{cases}$$

deflection different from 13° is penalized in objective function by following equation:

$$k_{up,down} = \left(\left|\delta_{up,down}\right| - 13\right)^2 \quad (2)$$

For this arrangement the weighting coefficients are:

$$a_1 = 1, a_2 = 5, a_3 = 0.2$$

Parameter vector **x** is contained in the space **P** with boundaries:

$$0.755 < e_X < 0.87$$
$$0.88 < f_X < 0.95$$
$$-0.2 < tan\,\gamma < 0.2$$
$$0.1 < t < 1$$
$$0.01 < q_{c\,up} < 0.3$$
$$-0.3 < q_{c\,down} < -0.01$$

Reserve factor is evaluated as:

$$RF_{up,down} = \max\left(\frac{\sigma_i}{\sigma_a}\right) \quad (3)$$

where σ_a = 200 MPa is allowable stress (same for tensile and compressive); σ_i is a von Mises stress on i-th element of the morphing skin.

Problem is solved on a 10 mm wide wing segment corresponding to 10 elements in span-wise direction. The chord length is 500 mm. All loads are distributed loads and distributed moments. Aerodynamic force on the flaperon and the morphing skin was estimated using the CS23 acceptable means of compliance (AMC) procedure for the wing loading 60 kg/m^2, the pressure loading of 376,6 Pa was applied on both the morphing skin and the rigid body of the flaperon. The aerodynamic force orientation was against the flaperon deflection, therefore necessitating increase of the control force. Self-weight was not included. Morphing skin material was isotropic with E = 6000 MPa, μ = 0.3. The elastic modulus resembles the low modulus GFRP.

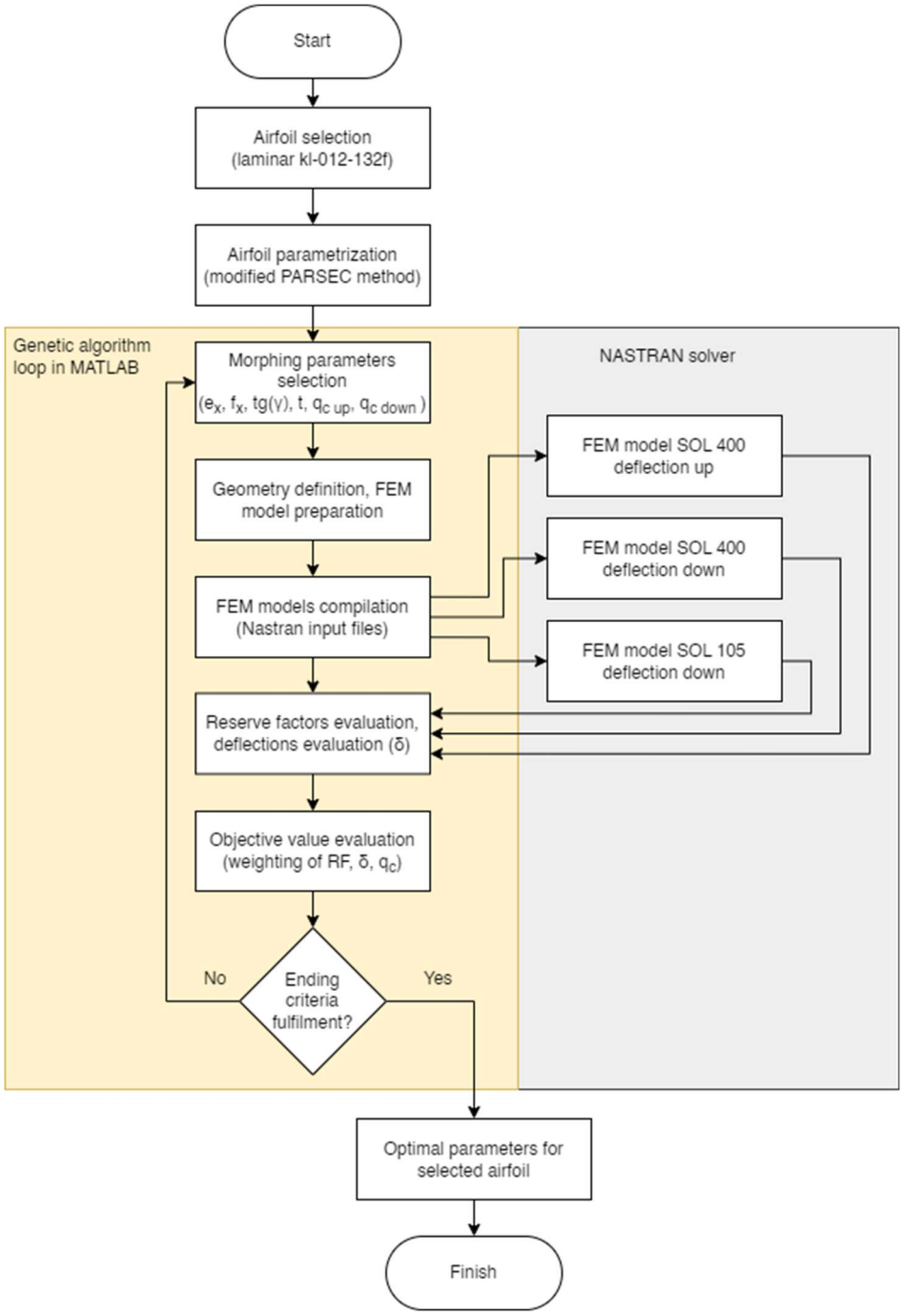

Figure 3 - Flowchart of the flaperon design using the GA

The optimization problem was solved using the MATLAB scripting with the build-in “ga” function. The whole algorithm arrangement can be seen in Figure 3. Before the optimization loop, the airfoil is parametrized by PARSEC method [12], which is modified to properly represent the flapped laminar airfoil. The stress and strain sub-analysis were calculated using the NASTRAN solver. The single objective value evaluation includes 3 different FEM calculations. The upper deflection used the SOL 400 with geometric nonlinearity for strain and stress calculation and therefore to evaluate the flaperon deflection. The lower deflection works similarly with opposite aerodynamic loading and control force orientation. Additionally, the SOL 105 for buckling factor was calculated for lower deflection. The stopping criteria is function tolerance $1 \cdot 10^{-4}$ and 5 stall generations.

5. Results

The result was obtained after evaluation of 12800 individuals (64 generations), where the objective value reached f=2.5371. The evolution is in Figure 4, higher values are cropped.

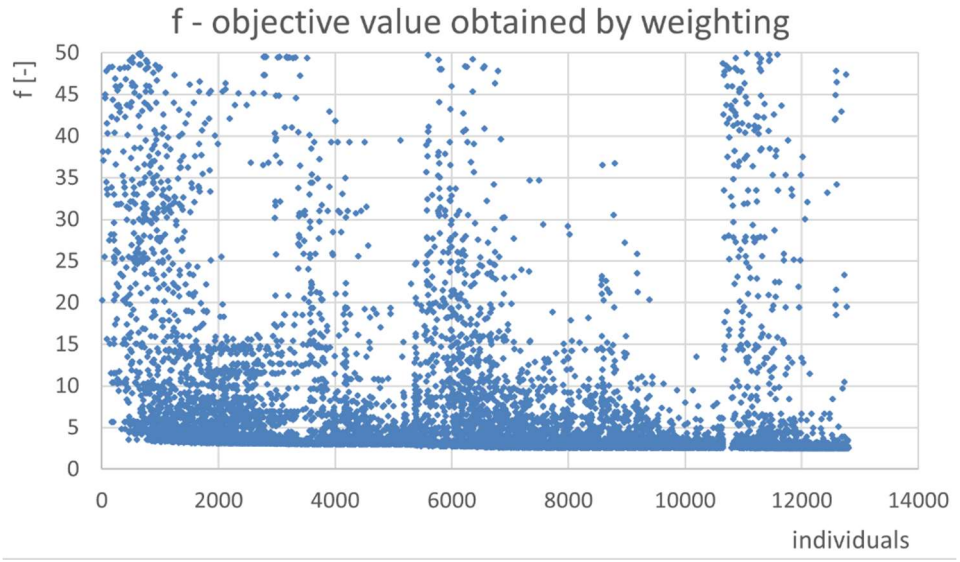

Figure 4 Evolution of the objective value f

The algorithm converges to a solution which defines a location, length and thickness of the morphing skin and the rail angle. For each individual subcase solution, the distributed control force and respective deflection is available for both upper and lower deflection. The genetic algorithm evolution of the parameters and the objective values can be seen in composed Figure 5. The 4 geometric parameters are in the left column, top to bottom. The control forces work as both parameters and objective values, they are located in the right column. Below them, there are reserve factors of the morphing skin for the upper and the lower deflections. In the bottom right-hand corner, there are achieved flaperon deflections. In the bottom left-hand corner, there are calculated eigenvalues – buckling safety factors.

The output geometry achieved by the best individual of the last generation is:

$$e_x = 0.758$$
$$f_x = 0.900$$
$$tan\,\gamma = -0.172$$
$$t = 0{,}28\ mm$$

The corresponding control forces are:

$$q_{c\,up} = 0.127\ N/mm$$
$$q_{c\,down} = -0.177\ N/mm$$

The reserve factor for the morphing deflection for up and down deflections:

$$RF_{up} = 0.422$$
$$RF_{down} = 0.509$$

The respective deflections are 13.02 up and -12.78 down.
The eigenvalue is negative: -2.21, the buckling does not occur under the current load orientation.

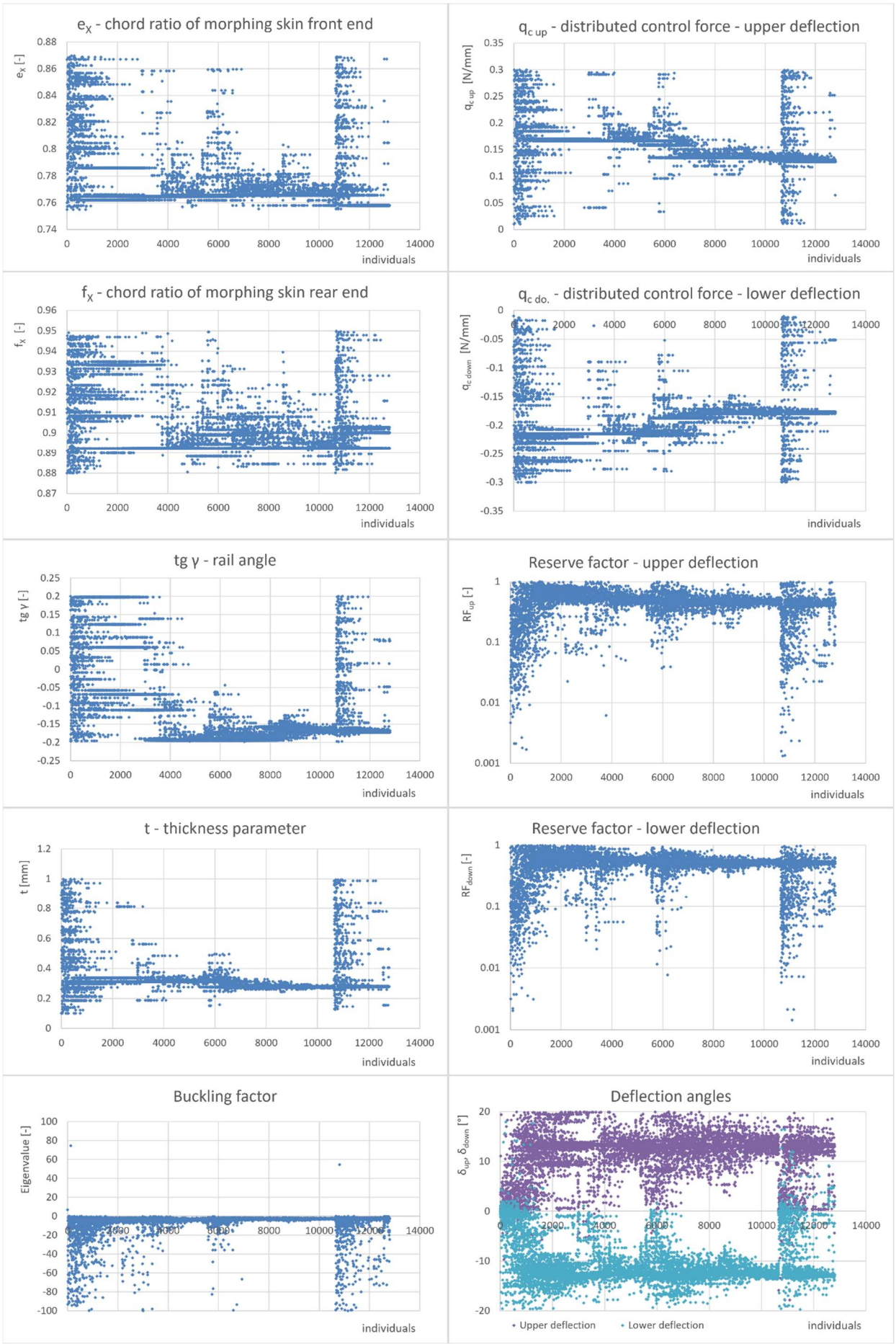

Figure 5 – Parameters (e_x, f_x, t, tg γ, $q_{c\,up}$, $q_{c\,down}$) and obj. values ($q_{c\,up}$, $q_{c\,down}$, RF_{up}, RF_{down}, δ_{up}, δ_{down})

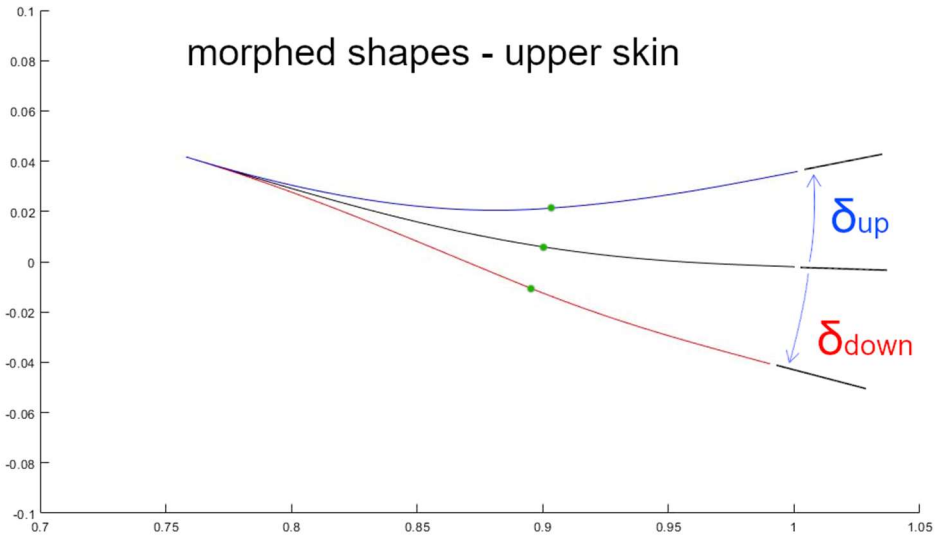

Figure 6 Airfoil trailing edge curves achieved by morphing skin and rigid flaperon (green points mark the divide)

The upper skin curves of the morphing skin and the rigid flaperon at full deflection obtained for the parameters described above can be seen in Figure 6. The S-shape in the lower deflection can be considered undesirable, but it is a consequence of the rigid trailing edge part and morphing motion. Based on the optimized geometry the mutual relationship of the required control force and deflection angle was calculated for the expected range of flaperon motion. In this case, the aerodynamic force is assumed to act against the deflection of the flaperon proportionally to the deflection angle. The full magnitude of aerodynamic force is used at ±13° (like in the optimization). This can be seen in Figure 7. The control force for flaperon deflection without aerodynamic forces was plotted for comparison.

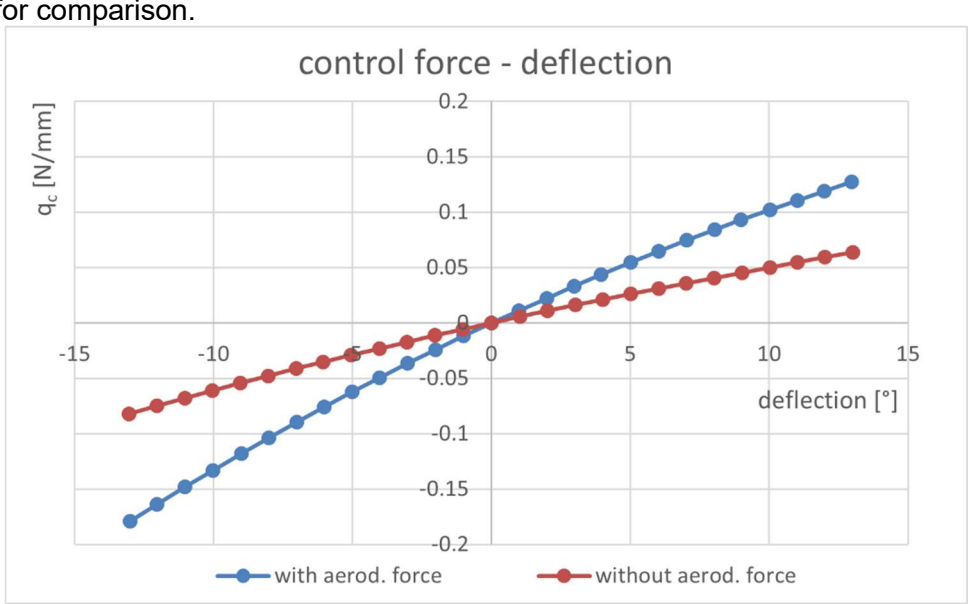

Figure 7 Control force required for deflection of flaperon, with and without aerodynamic force

6. Discussion

The input parameters reached the narrow bands during the evolution as well as the objective values, the problem is well conditioned. The difference of the optimized up and down deflection is caused by the objective function and weighting. The Figure 7 shows the control force gradient for upper and lower deflections. The control force gradient is higher for lower deflection and therefore the algorithm decides to leave the optimal deflection of -13° in order to decrease the control force. The morphing skin start and end locations show, that maximizing of the morphing skin length was not attempted. The front end of the morphing skin at the lower boundary can be explained by maximization of the force couple arm between morphing skin and hinge location. The rail angle is

negative and close to the boundary. The morphing skin thickness is rather low, but not at the lower boundary. This can be caused by the negative influence of the thin skin on the tensile load capacity.

The ratio of the control force and aerodynamic loads is approx. 1:1, the ratio can be seen in Figure 7, where subtracting the aerodynamic loads halves the required control force. This means the introduction of presented morphing arrangement requires approx. 2 times the force of the traditional hinged surface with control lever inside the airfoil contour. The increase is caused by the required deformation of the morphing skin. It points at the importance of control force reduction. But it must be remembered, that the aerodynamic load was obtained using simplified AMC procedure and may vary with actual airfoil pressure field. Translation of the hinge in the rail at full deflection of 13° is approx. 0.8% of the airfoil chord length, which is rather few. This might require higher manufacturing precision than usually.

7. Future research

The future research will focus on addressing of the effects that were omitted in the preliminary design, like fatigue properties of the morphing skin, actual stiffness of non-morphing parts, rail forces and the distribution of the shear force. The demonstrator of the arrangement will be developed. The options to improve the built-in regarding different airfoils will be investigated. To accelerate the optimization, it will be necessary to improve algorithm by structurization e.g., by iterative control force evaluation to make the connection of control force – deflection more obvious to the algorithm. Unfavorable S-shaped morphing skin in lower deflection can be observed in Figure 6. This is caused by initial airfoil shape in combination with morphing kinematics and needs attention in later development phase.

8. Conclusion

The problem formulation as presented proved feasible and the genetic algorithm is suitable for the solution. While the use of the threshold in constraints was rather effective for the reduction of weighting coefficients selection, the effects can still be observed in final deflections. Even after the control force optimization, the control force required for morphing skin deformation is relatively high. Despite the design originated from the sailplane technology development, the control force related problems might limit the use of the presented morphing flaperon arrangement for small scale aerial vehicles.

Contact Author Email Address

mailto: Lukas.Dubnicky@vutbr.cz

Copyright Statement

Acknowledgement

This work has been supported by the project No. FSI-S-23-8163 funded by The Ministry of Education, Youth and Sport (MEYS, MŠMT in Czech) institutional support.

References

[1] Barbarino S, Bilgen O, Ajaj R M, Friswell M I and Inman D J. A Review of Morphing Aircraft. *Journal of Intelligent Material Systems and Structures*, Vol. 22, No. 9, pp 823-877, 2011.

[2] Thill C, Etches J, Bond I, Potter K and Weaver P. Morphing skins. *The Aeronautical Journal*, Vol. 112, No. 1129, pp 117-139. 2008.

[3] Peel L D, Mejia J, Narvaez B, Thompson K and Lingala M. Development of a Simple Morphing Wing Using Elastomeric Composites as Skins and Actuators. *Journal of Mechanical Design,* Vol. 131, No. 9, 2009.

[4] Kensche H. Einige neue Konstruktionsrichtlinien fur den Bau von Leistungs-Segelfugzeugen. *Technical Soaring*, Vol. 3, No. 1, 1954.

[5] Thomas F and Laude J. Vergleichsmessungen an Laminarflugeln mit starrer und flexibler Wolbungsklappe. *Technical Soaring*, Vol. 10, No. 1, 1968.

[6] Heintz C. Design and Application of the ZODIAC's Hingeless Aileron. *Zenair Newsletter*. 1999.

[7] Wu R, Soutis C, Zhong S and Filippone A. A morphing aerofoil with highly controllable aerodynamic performance. *The Aeronautical Journal*, Vol. 121, No. 1235, pp 54-72, 2017.

[8] Cheng G, Ma T, Yang J, Chang N and Zhou X. Design and Experiment of a Seamless Morphing Trailing Edge. *Aerospace,* Vol. 10, no. 3, 2023.

[9] Achleitner J, Rohde-Brandenburger K, Rogalla von Bieberstein P, Sturm F and Hornung M. Aerodynamic Design of a Morphing Wing Sailplane. *AIAA Aviation 2019 Forum*, 2019.

[10] Sturm F, Achleitner J, Jocham K and Hornung M. Studies of Anisotropic Wing Shell Concepts for a Sailplane with a Morphing Forward Wing Section. *AIAA Aviation 2019 Forum*, 2019.

[11] Kubrynski K. Design of a Flapped Laminar Airfoil for High Performance Sailplane. *30th AIAA Applied Aerodynamics Conference*, 2012.

[12] Sobieczky H. Parametric Airfoils and Wings. *Recent Development of Aerodynamic Design Methodologies,* pp 71-87, 1999.